Silencing of UTX Mitigates Aging-Associated Cardiac Fibrosis via Blocking Cardiac Fibroblasts-to-Myofibroblasts Trans-Differentiation

ABSTRACT

Background: Cardiac fibrosis increases with age. Fibroblast activation plays an essential role in cardiac fibrosis. Histone modifications are involved in various chromatin-dependent processes. Attenuation of the histone H3 trimethylation on lysine 27 demethylase UTX by RNA interference or heterozygous mutation extends lifespan in worm. The objective of this study was to explore whether epigenetic silencing of UTX mitigates aging-associated cardiac fibrosis.

Methods: Middle-aged mice (15 months old) were used and started to receive adeno-associated virus-scrambled-small hairpin RNA and adeno-associated virus-UTX-small hairpin RNA every 3 months from 15 months to 21 months, respectively. The mice were euthanized at 24 months of age (length of the study).

Results: Adeno-associated virus-UTX-small hairpin RNA delivery significantly attenuated aging-associated increase in blood pressure, especially in diastolic blood pressure, indicating silencing of UTX rescued aging-associated cardiac dysfunction. Aging-associated cardiac fibrosis is characterized by fibroblast activation and abundant extracellular matrix deposition, including collagen deposition and alpha smooth muscle actin activation. Silencing of UTX abolished collagen deposition and alpha smooth muscle actin activation, decreased serum transforming growth factor β, blocked cardiac fibroblasts-to-myofibroblasts trans-differentiation by elevation of cardiac resident mature fibroblast markers, TCF21, and platelet-derived growth factor receptor alpha, which are important proteins for maintaining cardiac fibroblast physiological function. In the mechanistic study, adeno-associated virus-UTX-small hairpin RNA blocked transforming growth factor β-induced cardiac fibroblasts-to-myofibroblasts trans-differentiation in isolated fibroblasts from 24-month-old mouse heart. The same results demonstrated as the *in vivo* study.

Conclusions: Silencing of UTX attenuates aging-associated cardiac fibrosis via blocking cardiac fibroblasts-to-myofibroblasts trans-differentiation and consequently attenuates aging-associated cardiac dysfunction and cardiac fibrosis.

Keywords: UTX/KDM6A, fibrosis, shRNA, fibroblast, myofibroblast, cardiac

INTRODUCTION

Epigenetic modifications play an essential role in the physiological and pathological events of organisms and contribute to the regulation of cell fate, the maintenance of cell specificity, and cell-type-specific functions.[1,2] The role of histone modifications in the process of aging has emerged, providing insights into epigenetic mechanisms of aging and lifespan regulation.[3,4] Ubiquitously transcribed tetratricopeptide repeat on X chromosome (UTX)/lysine demethylase 6A (KDM6A) is a histone demethylase enzyme responsible for removing the methyl group of histone H3 trimethylation on lysine 27 (H3K27me3)/H3K27me2 to initiate the transcription of target genes.[5] The loss of H3K27me3 and the increased activity of the H3K27 demethylase UTX occur during aging.[6] Silencing of UTX-1 gene extended the mean life span of *C. elegans*.[3] A premature aging disease Hutchinson—Gilford Progeria Syndrome (HGPS) has been reported to be associated with the loss of H3K27me3.[7,8] However, the role of UTX in the regulation of aging-associated cardiac fibrosis remained unclear.

Chao Li (ID)
Tiantian Lin (ID)
Delin Li (ID)
Daoyuan Si (ID)
Huan Sun (ID)
Sibao Yang (ID)
Zhongfan Zhang (ID)
Qian Zhang (ID)
Kaiyao Shi (ID)

Department of Cardiology, Jilin Provincial Molecular Biology Research Center for Precision Medicine of Major Cardiovascular Disease, Jilin Provincial Cardiovascular Research Institute, China-Japan Union Hospital of Jilin University, Jilin, China

Corresponding author:
Kaiyao Shi
✉ shiky@jlu.edu.cn

Anatol J Cardiol 2023; 27(7): 398-407

Li et al. Silencing of UTX and Cardiac Fibrosis

Aging is associated with increased cardiac interstitial fibrosis and diastolic dysfunction.[9] Fibroblasts are found throughout the cardiac tissue and play an important role in the secretion of extracellular matrix (ECM). They are not terminally differentiated and can be activated by a variety of chemical signals that promote proliferation and cellular differentiation to form myofibroblasts with an upregulated rate of matrix production.[10,11] Fibroblast content increases with aging[12,13] and associates with increased cross-linking of collagen, contributing to diastolic dysfunction. Upon the activation of fibroblasts, transcription factor 21 (TCF21) and platelet-derived growth factor receptor alpha (PDGFRα) are reduced, and alpha smooth muscle actin (αSMA) is upregulated in resident cardiac fibroblasts.[14] Transcription factor 21 is crucial for the development of a number of cell types during embryogenesis of the heart.[15] The activation of TCF21 is directed by TARID (TCF21 antisense RNA-inducing demethylation). TARID activates TCF21 expression by inducing promoter demethylation and affects expression levels of target genes by functioning as epigenetic regulators of chromatin structure through interactions with histone modifiers, chromatin remodeling complexes, transcriptional regulators, and/or DNA methylation machinery.[16] Platelet-derived growth factor receptor alpha is an important factor for maintaining cardiac fibroblast function. Mutational activation of PDGFRα systemically induced fibroblastic hyperplasia and increased ECM deposition.[17]

However, the relations of UTX and TCF21/PDGFRα in cardiac fibroblast activation and transition into the myofibroblast remained to be investigated. Here we used adeno-associated virus 2/9 (AAV2/9) to deliver UTX-shRNA into aged mice to prevent cardiac fibroblast activation and fibrosis. Our work reveals an epigenetic function of UTX in regulation of aging-associated cardiac fibrosis via cardiac fibroblasts-to-myofibroblasts trans-differentiation.

HIGHLIGHTS

- Silencing of ubiquitously transcribed tetratricopeptide repeat on X chromosome (UTX) attenuates cardiac fibrosis via blocking cardiac resident fibroblasts-to-myofibroblasts trans-differentiation both *in vivo* and ex vivo.
- We revealed an epigenetic regulation of UTX on aging-associated cardiac hypertrophy and fibrosis using an AAV as a vector to deliver utx-shRNA.
- A UTX-specific target histone H3 was upregulated in both heart tissue and isolated cardiac fibroblasts, indicating that UTX protein was silenced efficiently.
- Silencing of UTX abolished myofibroblast markers, type I collagen and αSMA expression, and upregulated TCF21 and PDGFRα expression.
- The AAV-utx-shRNA significantly attenuated the aging-associated increase in BP and blocked fibroblasts-to-myofibroblasts trans-differentiation.

METHODS

Construction of Recombinant Adeno-associated Virus

Two mouse UTX (ACCESSIONNM_009483) shRNAs (Table 1) were designed using Biosettia's software (San Diego, CA) and synthesized by SBS Genetech (Beijing, China). The recombinant AAV vector with utx-shRNAs (Supplementary Figure 1A-B and Table 1) and scrambled (SC) shRNA (Supplementary Figure 1C) were constructed by inserting the shRNAs into AAV vector (Supplementary Figure 1A). The AAVs were packaged in AAV/293 cells by co-transfection of AAV9-rep and cap (Supplementary Figure 1D) and helper (Supplementary Figure 1E). For AAV purification, iodixanol density gradient centrifugation method was used.[18] The titer was determined by real-time polymerase reaction (RT-PCR) as described by Rohr et al.[19] The inhibition efficiency was tested in isolated cardiac fibroblast cells. One of the utx-shRNAs (Supplementary Figure 1B) with greater inhibition efficiency was chosen for the *in vivo* and *ex vivo* studies.

Animal Study

All mice were housed at room temperature for 12 hours dark and 12 hours light throughout the experiment. Twelve male C57BL/6J mice (15 months old) were used in this study. Blood pressure (BP) was measured monthly using the tail-cuff method[20] (CODA6 BP monitoring system, Kent Scientific). At ages of 15, 18, and 21 months, 6 mice received AAV-utx-shRNA and 6 mice received AAV-sc-shRNA, respectively. The AAVs were delivered intravenously via tail vein at 2×10^9 genomic particles (GP)/100 μL per mouse. All mice euthanized at the end of 9 months after AAV delivery (24 months old, the length of the study).

Isolation of Cardiac Fibroblasts and Myofibroblast Induction

Cardiac fibroblasts were isolated according to the protocol.[21] Briefly, the hearts were rapidly excised from anesthetized mice (24-month-old C57BL/6J) with over dose pentobarbital (200 mg kg IP), minced and placed in a collagenase/pancreatin digestion solution (80 units/mL and 0.6 mg/mL, respectively). After four 20-min collagenase/pancreatin digestions in a balanced salt solution (6.8 g/L NaCl, 0.4 g/L KCl, 0.1 g/L $MgSO_2$, 0.12 g/L NaH_2PO_4, 4.76 g/L HEPES, 1.0 g/L D-glucose, 0.02 g/L phenol red, pH 7.4), the accumulated cells were subjected to Percoll gradient centrifugation. The fibroblasts were collected from nonmyocyte cell band (mostly fibroblasts). The cells were washed twice with Dulbecco's modified Eagle's medium (DMEM) plus penicillin/streptomycin/fungizone (PSF) and cultured in DMEM supplemented with PSF and 10% fetal bovine serum (FBS). The cells were then plated onto uncoated cell culture dishes for 30 minutes. This initial plating step allowed for the preferential attachment of fibroblasts to the bottom of the culture dish. Nonadherent or weakly adherent cells were removed, fresh medium was added, and cells were allowed to grow until confluence and subsequently passaged. Cell passage was performed with a trypsin-ethylenediaminetetraacetic acid (EDTA) solution. Cardiac fibroblasts were permitted to grow to the desired confluence. All cells used in these experiments were from passages 0 through 1. To induce myofibroblasts, 5 ng/mL

Li et al. Silencing of UTX and Cardiac Fibrosis

Anatol J Cardiol 2023; 27(7): 398-407

Table 1. Two UTX shRNA Sequences

Utx-shRNA-1,5'-AAAAGGCGTTGGAGTTGTGAATTTTGGATCCAAAATTCACAACTCCAACGCC-3'	
Utx-shRNA-2,5'-AAAAGCTGTTCGCTGCTACGAATTTGGATCCAAATTCGTAGCAGCGAACAGC-3'	
AAAA, overhang	
TTGGATCCAA, loop	
Utx-shRNA-1	401-419, 5' utr (-31nt~-13nt), 5' UTR, GC content, 47.37 %
Utx-shRNA-2	663-681, exon 2 (+231nt~+249nt), GC content, 52.63 %

transforming growth factor β (TGFβ) (R&D, 7666-MB-005) was added to the culture medium and cultured for 5 days.

Cell Culture and Transfection

The isolated cells were seeded in a six-well plate at 1×10^5 cells/well, cultured in conditions of Roswell Park Memorial Institute (RPMI) 1640 (Gibco,Missoula, Montana, USA) with 10% FBS and 100 U/mL penicillin supplemented at 37° with 5% CO_2 in a humidified atmosphere and incubated overnight. Five micrograms of pAAV-SC-shRNA (control) and 5 μg of pAAV-UTX-shRNAs were diluted in 50 μL of Opti transfection medium, meanwhile, diluted 10 μL of lipofectamine 2000 in 50 μL of Opti transfection medium. After 5 minutes of incubation, the diluted DNA was combined with diluted Lipofectamine 2000 (total volume = 100 μL). This was mixed gently and incubated for 20 minutes at room temperature.

Then, 100 μL of complexes was added to each well containing cells and medium. This was mixed gently by rocking the plate back and forth. The medium was refreshed after incubation at 37° with 5% CO_2 in a humidified atmosphere for 6 hours. The transfected cells were cultured for addition 48 hours, and then the cells were harvested for Western blot and RT-PCR.

Histological Staining

The hearts from euthanized mice were collected and fixed with 4% paraformaldehyde (PFA). Paraffin-embedded tissues were sectioned (5 μm) and used for the staining. Collagen deposition was evaluated by Sirius red (Abcam, ab150681) and Masson Trichrome (Sigma, HT15-1KT,St. Louis, MO, USA) staining kit. All procedures were performed according to the manual instructions.
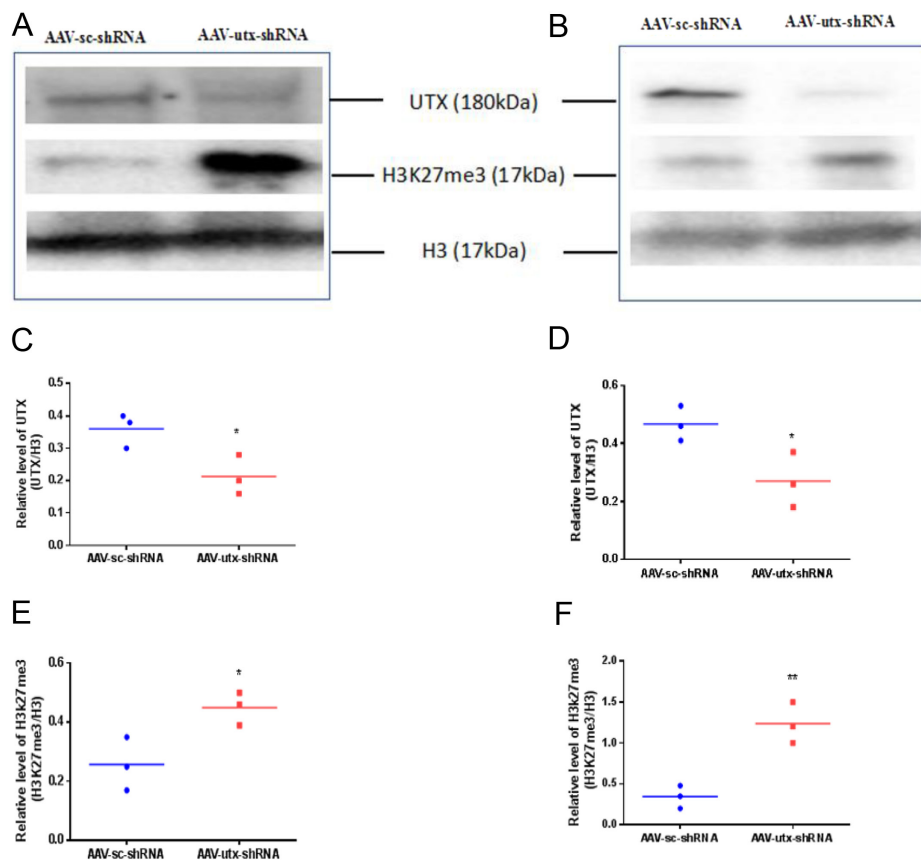

Figure 1. AAV-utx-shRNA delivery abolished UTX expression and promotes H3K27me3 expression in the heart tissue and isolated cardiac fibroblasts. A, C, and E: Western blot analysis of UTX and H3K27me3 expression in the heart tissue. n = 3. B, D, and F: Western blot analysis of UTX and H3K27me3 expression in the isolated cardiac fibroblasts. n = 3. Data are expressed as mean ± SEM. *P < .05, **P < .01 (n = 3) vs. AAV-sc-shRNA-treated control mice. AAV, adeno-associated virus; H3K27me3, histone H3 trimethylation on lysine 27; shRNA, short hairpin RNA; UTX, ubiquitously transcribed tetratricopeptide repeat on X chromosome.

Western Blot Analysis

Western blot analysis was carried out as described previously.[22] Briefly, membrane was blocked with 5% bovine serum albumin (BSA) for 60 minutes at room temperature, then incubated with mouse anti-UTX (CST Danvers, MA, USA, 1 : 1000), mouse anti-PDGFRα (Santa Cruz, 1:1000), rabbit anti-TCF21 (Aviva Systems Biology, 1 : 1000), αSMA (Abcam, 1:2000), glyceraldehyde 3-phosphate dehydrogenase (GAPDH) (Proteintech, 1:2000), and histone H3 (CST, 1 : 2000). Goat anti-rabbit or goat anti-mouse conjugated with horseradish peroxidase (Santa Cruz, 1:2000) was used as the secondary antibodies and incubated for 1 hour at room temperature. After washing with 1× TBST between antibody incubations, protein bands were developed in enhanced chemiluminescence and the density was quantified using Image J software.

Measurement of Mouse Serum Transforming Growth Factor β by ELISA

Mouse serum TGFβ was measured by ELISA (Abcam, ab119557) according to the manufacture's instruction.

Table 2. Primer List for Real-time RT-PCR

| Gene Name	Accession#	Primer Sequence
PDGFRα	NM-011058	Forward,5'-CTCGTGCTTGGTCGGATTT-3' Reverse,5'-TCTTCACAGCCACCTTCATTAC-3'
TCF21	NM-011545	Forward,5'-GACAAGTACGAGAACGGTTACA-3' Reverse,5'-ACCACTTCCTTCAGGTCATTC-3'
αSMA	NM-007392	Forward,5'-GACTCTCTTCCAGCCATCTTTC-3' Reverse,5'-GACAGGACGTTGTTAGCATAGA-3'
GAPDH	NM-001411842	Forward,5'-AACAGCAACTCCCACTCTTC-3' Reverse,5'-CCTGTTGCTGTAGCCGTATT-3'

RT-PCR, real-time polymerase reaction.
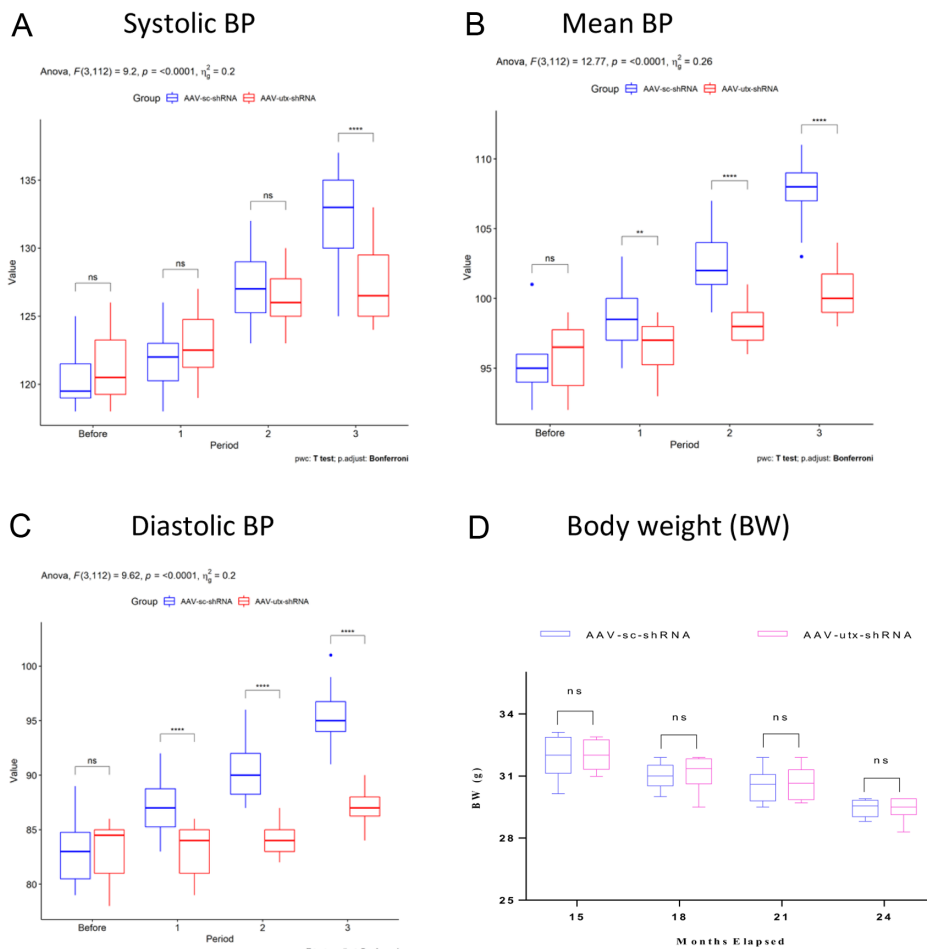
Figure 2. Silencing of UTX reduced aging-associated increase in BP. BP was measured monthly by the tail-cuff method using a CODA 6 BP monitoring system during the administration of AAV-utx-shRNA and AAV-sc-shRNA. (A): Changes in systolic BP with age. (B): Changes in mean BP with age. (C): Changes in diastolic BP with age. (D): Changes in body weight with age. Data were expressed as mean ± SEM. *P < .05, **P < .01, ***P < .001 (n = 6) vs. AAV-sc-shRNA-treated control mice. AAV, adeno-associated virus; BP, blood pressure; shRNA, short hairpin RNA; UTX, ubiquitously transcribed tetratricopeptide repeat on X chromosome.

Li et al. Silencing of UTX and Cardiac Fibrosis

Anatol J Cardiol 2023; 27(7): 398-407

Real-Time Polymerase Chain Reaction

Cardiac fibroblasts were isolated from 24-month-old mice. The cells were transfected with AAV-sc-shRNA and AAV-utx-shRNA for 48 hours and treated with TGFβ for additional 72 hours. Total RNA was extracted using TRIzol (Invitrogen,Waltham, MA, USA) as per the manufacturer's instructions. cDNA was synthesized from 2 μg of total RNA with QuantiTech reverse transcription kit (Cat. #, 205311, Qiagen). The appropriate primers (Table 2) were designed with DTDNA Primer Quest tool. Along with PowerTrack SYBR-Green Master Mix (cat. #, A46012, Fisher) and a total of 0.1 μg cDNA, they all used for real-time PCR reaction. The reactions were performed in 3 technical and 3 biological repeats to enable reliable statistical analysis. The Applied Biosystems Studio Quant 3 Real-Time PCR System was used, and the PCR program was 40 cycles of 15 seconds at 95° and 1 minute at 55° according to the manufacturer's instructions. ΔCT was obtained from target gene CT minus control CT, and ΔΔCT was calculated by subtracting the control mean ΔCT from each ΔCT. Comparative ΔΔCT was used for data analysis, and calculations were made by $2^{-ΔΔCT}$ as the relative mRNA expression.

Statistical Analysis

Quantitative data were presented as mean ± SEM. The Kolmogorov–Smirnov test and Shapiro–Wilk test were used to perform the normality testing. All data passed the normality test. Data for BP were analyzed using the repeated-measures analysis of variance (2-group, 3-period measurement ANOVA) followed by the Bonferroni test. The remaining data (2 groups on a single period) were using the independent samples t-test. $P < .05$ was considered statistically significant.

RESULTS

Screening the Inhibition Efficiency of pAAV-utx-shRNAs in Isolated Cardiac Fibroblasts

Two pAAV-utx-shRNAs (Table 1) were tested in isolated cardiac fibroblasts from 24-month-old mice. Forty-eight hours after transfection of pAAV-utx-shRNAs, the cells were harvested and protein was extracted. The expression of UTX was evaluated by WB. The shRNA targets on Exon 2 (+231 nt ~ +249 nt) of utx gene showed greater inhibition (Supplementary Figure 2). Thus, we packaged this shRNA into AAV for the *in vivo* study.

AAV-utx-shRNA Delivery Abolishes UTX Expression in the Heart Tissue and Isolated Cardiac Fibrosis

To confirm the silencing of UTX by AAV-utx-shRNA *in vivo*, the hearts were collected from euthanized AAV-utx-shRNA and AAV-sc-shRNA-treated (control) mice. Cardiac fibroblasts were isolated for evaluation of UTX expression. The UTX protein was knocked down in both heart tissue (Figure 1A and 1C, $P < .05$) and isolated cardiac fibroblasts (Figure 1B and 1D, $P < .05$) in AAV-utx-shRNA-treated mice. In contrast, H3K27me3, a UTX-specific target histone H3, was upregulated in both heart tissue (Figure 1A and 1E, $P <$
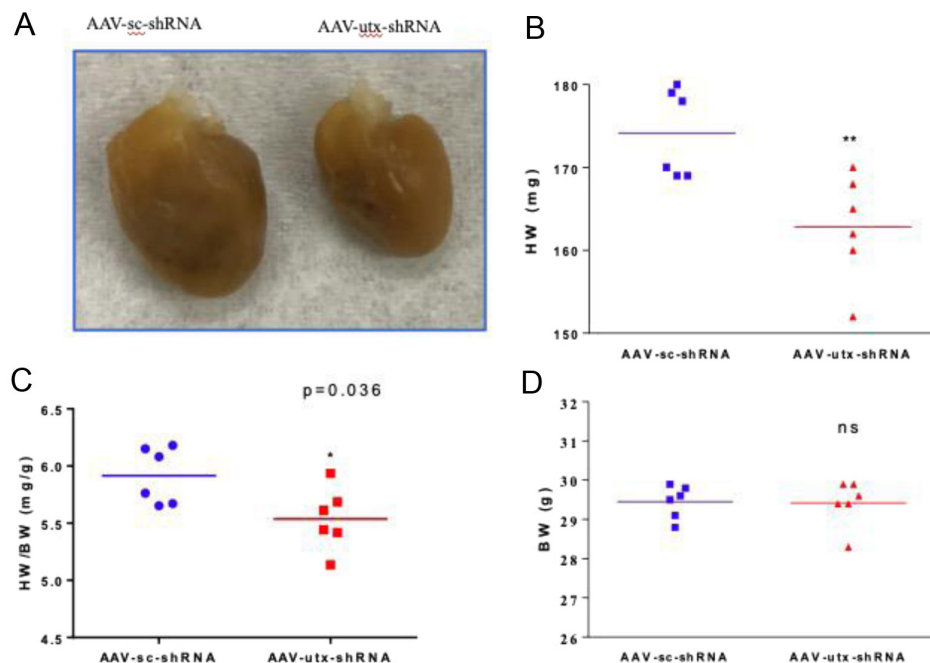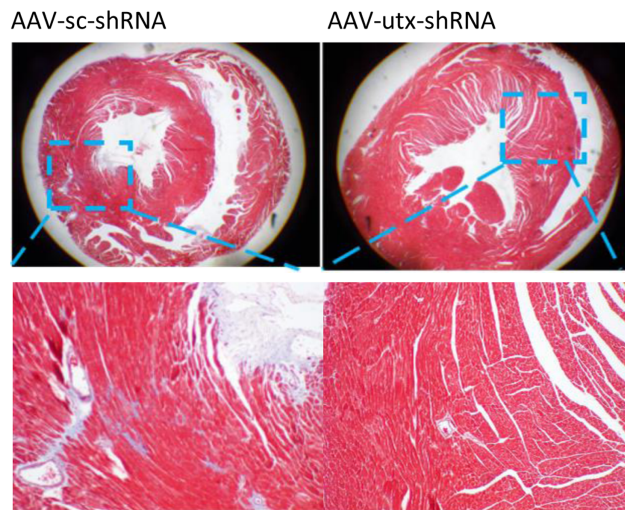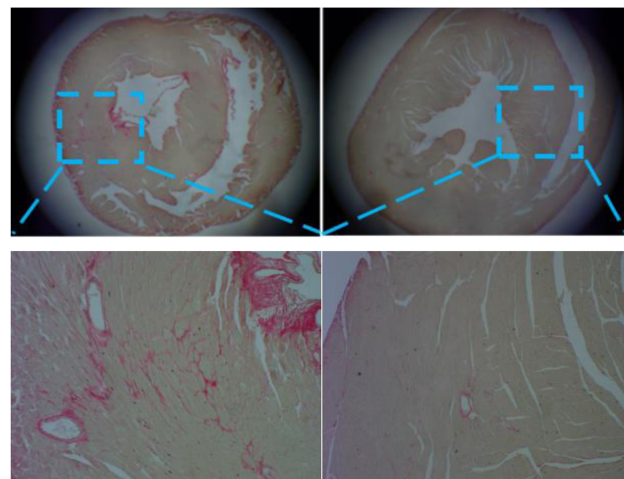

Figure 3. Silencing of UTX attenuated aging-associated heart hypertrophy. The hearts were dissected from euthanized mice with over-dose pentobarbital by IP at the age of 24 months after 9-month treatment with AAV-utx-shRNA or AAV-sc-shRNA. (A): Representative photographs showing the macroscopic features of aging-associated hypertrophic heart (left). AAV-utx-shRNA delivery abolished cardiac hypertrophy (right). (B): Heart weight (mg), n = 6. (C): The ratio of heart weight (mg) normalized with body weight (BW, g), n = 6. (D): BW, n = 6. Data are expressed as mean ± SEM. *P < .05, **P < .01 vs. AAV-sc-shRNA-treated control mice. AAV, adeno-associated virus; BW, body weight; shRNA, short hairpin RNA; UTX, ubiquitously transcribed tetratricopeptide repeat on X chromosome.
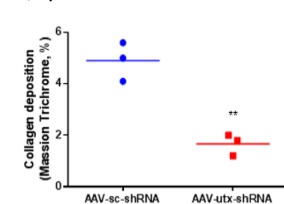
Anatol J Cardiol 2023; 27(7): 398-407

Li et al. Silencing of UTX and Cardiac Fibrosis

A, Representative Masson Trichrome staining

AAV-sc-shRNA   AAV-utx-shRNA
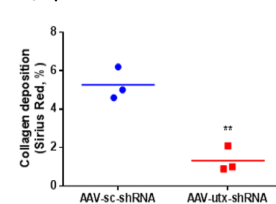

B, Representative Sirius Red staining

C, quantification for A   D, quantification for B
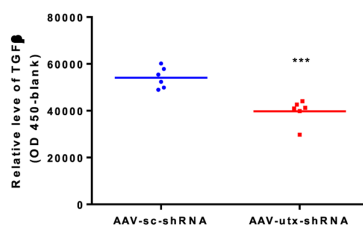

E, Serum TGFβ levels

Figure 4. Silencing of UTX abrogated the increase in aging-associated cardiac fibrosis. (A): Representative Masson Trichrome staining. Magnification, upper panel (×20) and bottom panel (×100). (B): Representative Sirius Red staining.

.01) and isolated cardiac fibroblasts (Figure 1B and 1F, $P < .05$), indicating that UTX protein was silenced efficiently.

Silencing of UTX Reduces Aging-Associated Increase in BP

Blood pressure is elevated with aging.[23] The systolic dysfunction becomes apparent at 18 months of age. These aging animals had left ventricular hypertrophy and fibrosis.[24] To explore the role of UTX in regulation of BP during the mouse life span (the length of the study), 12 C57BL/6J mices (15 months old) were used in the study. AAV-utx-shRNA delivery significantly reduced the aging-associated increase in systemic BP at 24 months. After 9 months 3-doses AAV-utx-shRNA administration, systolic(Figure 2A, $P = .001$), diastolic (Figure 2C, $P < .0001$), and mean (Figure 2B, $P < .01$) BP of mice were all lower than age-matched controls which were treated with AAV-sc-shRNA, indicating that silencing of UTX attenuated aging-associated BP elevation. Although AAV-utx-shRNA delivery did not alter body weight (BW) (Figure 2D, $P > .05$).

Silencing of UTX Attenuates Aging-associated Heart Hypertrophy

Aging is associated with an increased incidence of heart failure companying with heart hypertrophy, which is characterized by the loss in muscle mass and increase in myocyte cell volume per nucleus in both ventricles.[25] To evaluate whether silencing of UTX attenuates aging-associated cardiac hypertrophy, the hearts were dissected, weighed, photographed, and normalized with the BW. As shown in Figure 3, AAV-utx-shRNA delivery significantly attenuated aging-associated cardiac hypertrophy (Figure 3A) although AAV-utx-shRNA delivery did not change the BW (Figure 3D). Photograph images represented a hypertrophic heart in AAV-sc-shRNA-treated mice (Figure 3A left) while silencing of UTX lessened cardiac hypertrophy (Figure 3A right). The decrease in heart hypertrophy was represented in heart weight (Figure 3B, $P < .01$). To exclude the effect of BW, the heart weight was still obviously lower in AAV-utx-shRNA-treated mice after normalizing with the BW (Figure 3C, $P < .05$). These results suggest that UTX plays an important role in aging-associated cardiac hypertrophy.

Silencing of UTX Abrogates the Increase in Aging-associated Cardiac Fibrosis

Fibrosis occurs with aging.[26] Fibroblast is a type of biological cells that synthesizes the ECM and collagen.[27] To unravel the role of UTX in age-related cardiac fibrosis, we administrated mice starting from middle age (15 months old) to old age (24 months old) with AAV-utx-shRNA every 3 months and detected the outcome of 3 doses of utx-shRNA delivery. As

Magnification, upper panel (×20) and bottom panel (×100). (C): Quantification for (A) from ×100 images of Masson Trichrome staining, n = 3. (D): Quantification for (B) from ×100 images of Sirius Red staining, n = 3. (E): Serum TGFβ levels, n = 6. Data are expressed as mean ± SEM. **$P < 0.01$, ***$P < .001$ vs. AAV-sc-shRNA-treated control mice. AAV, adeno-associated virus; shRNA, short hairpin RNA; TGFβ, transforming growth factor beta; UTX, ubiquitously transcribed tetratricopeptide repeat on X chromosome.

depicted in Figure 4, AAV-utx-shRNA significantly reduced cardiac fibrosis (Figure 4A-D) and decreased serum TGFβ (Figure 4E, $P < .001$). Morphologically, the heart from AAV-sc-shRNA-treated mice (controls) represented large amount of collagen deposition by Trichrome Masson's stain (Figure 4A left) and Sirius Red stain (Figure 4B left) while aging-associated cardiac collagen deposition was depleted by AAV-utx-shRNA treatment (Figure 4A right and Figure 4B right). Quantitative data for Trichrome Masson's stain were shown in Figure 4C ($P < .01$), for Sirius Red stain, it was shown in Figure 4D ($P < .01$), indicating epigenetic modification of UTX-regulated cardiac remodeling.
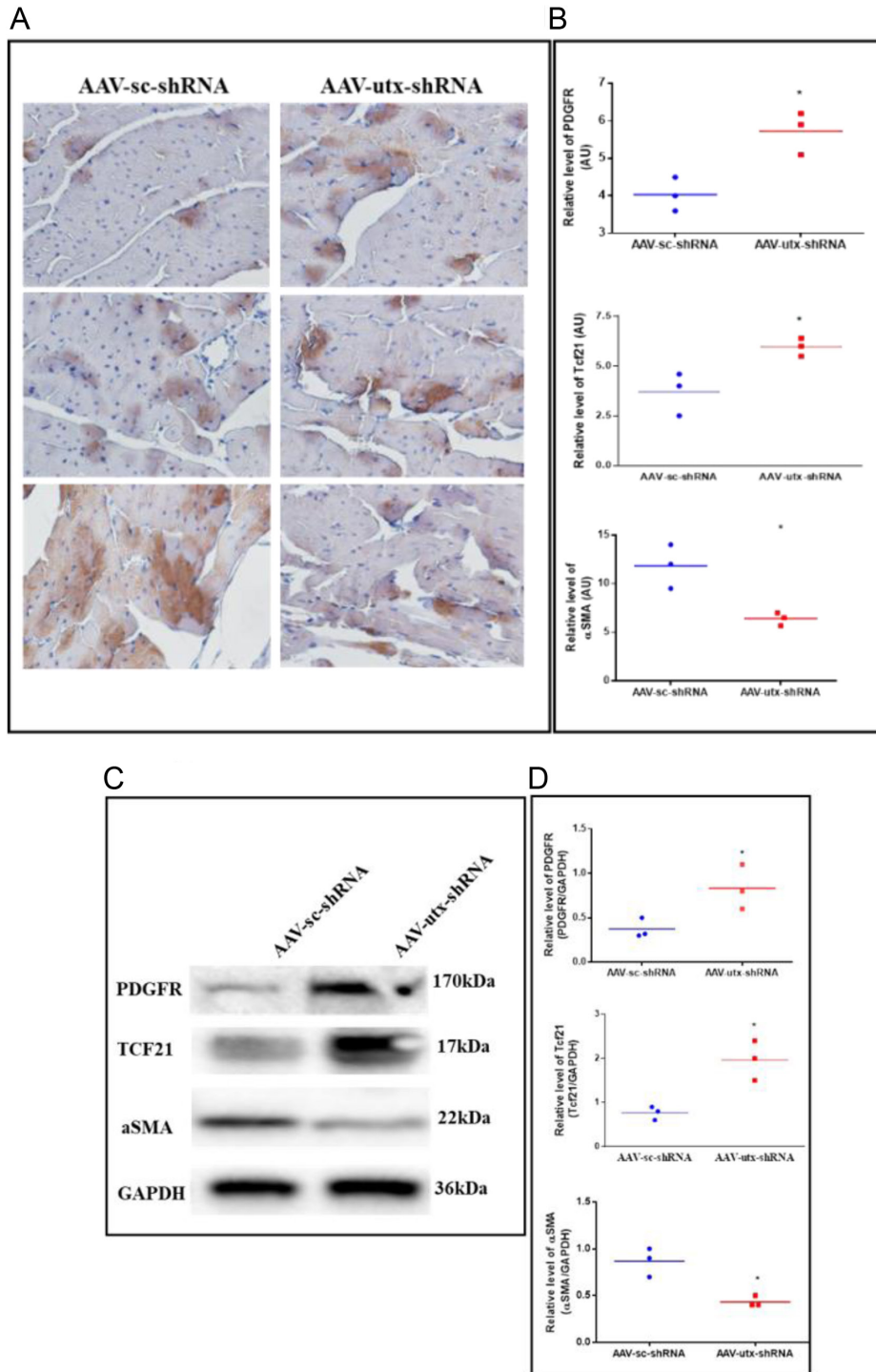

Figure 5. AAV-utx-shRNA blocked fibroblasts-to-myofibroblasts trans-differentiation. (A): Representative immunohistochemical staining of PDGFRα (upper panel), TCF21 (middle), and αSMA (bottom). (B): Quantification for (A). (C): Representative western blot analysis of PDGFRα (upper panel), TCF21 (middle), and αSMA (bottom). (D): Quantification for (C). Data are expressed as mean ± SEM. *$P < .05$ vs. AAV-sc-shRNA-treated control mice, n = 3. AAV, adeno-associated virus; PDGFRα, platelet-derived growth factor receptor alpha; αSMA, alpha smooth muscle actin; TCF21, transcription factor 21; shRNA, short hairpin RNA.

Silencing of UTX Blocked Cardiac Fibroblast Activation *In vivo* and *Ex vivo*

Next, we investigated the mechanism of how UTX regulates aging-associated cardiac fibrosis. The previous report showed that nonactivated cardiac fibroblasts, known as mature cardiac fibroblasts, express PDGFRα and TCF21, but do not express αSMA.[16] Activation of cardiac fibroblasts results in abundant ECM, including collagen I and αSMA expression. The expression of PDGFRα and TCF21 was reduced along with the cardiac fibroblast activation.[28] To evaluate the role of UTX in cardiac fibroblast activation in aged mouse heart, PDGFRα, TCF21, and αSMA were detected in heart tissue (24 months old) by both IHC (Figure 5A) and WB (Figure 5C). As shown in Figure 5, IHC data showed that silencing of UTX increased mature cardiac fibroblasts markers, PDGFRα (Figure 5A and Figure 5B upper panel, $P < .05$) and TCF21 (Figure 5A and Figure 5B middle panel, $P < .05$), and decreased the activation marker, αSMA, expression (Figure 5A and Figure 5B bottom panel, $P < .05$). Similarly, WB results were consistent with IHC results, in which PDGFRα (Figure 5C and Figure 5D upper panel, $P < .05$) and TCF21 (Figure 5C and Figure 5D middle panel, $P < .05$) decreased

the activation marker αSMA expression (Figure 5C and Figure 5D lower panel, $P < .05$). Glyceraldehyde 3-phosphate dehydrogenase serves as the internal control (Figure 5C, bottom panel). In isolated cardiac fibroblasts, AAV-utx-shRNA blocked TGFβ-induced increase in αSMA (Figure 6C, $P < .01$) and decrease in PDGFRα (Figure 6A, $P < .01$) and TCF21 (Figure 6B, $P < .001$). These data suggest that silencing of UTX blocks cardiac fibroblasts-to-myofibroblasts trans-differentiation.

DISCUSSION

This study is the first to show that silencing of UTX attenuates cardiac fibrosis via blocking cardiac resident fibroblasts-to-myofibroblasts trans-differentiation. This is supported by both *in vivo* and *ex vivo* studies presented here.

Under physiological conditions, cardiac fibroblasts express no stress fibers. After injury, however, fibroblasts are activated and transdifferentiate into stress-fiber expressing myofibroblasts.[29,30] The 2 cardiac resident mature fibroblast markers, TCF21 and PDGFRα are important proteins for maintaining cardiac fibroblast physiological function while stress protein including type I collagen and αSMA express in
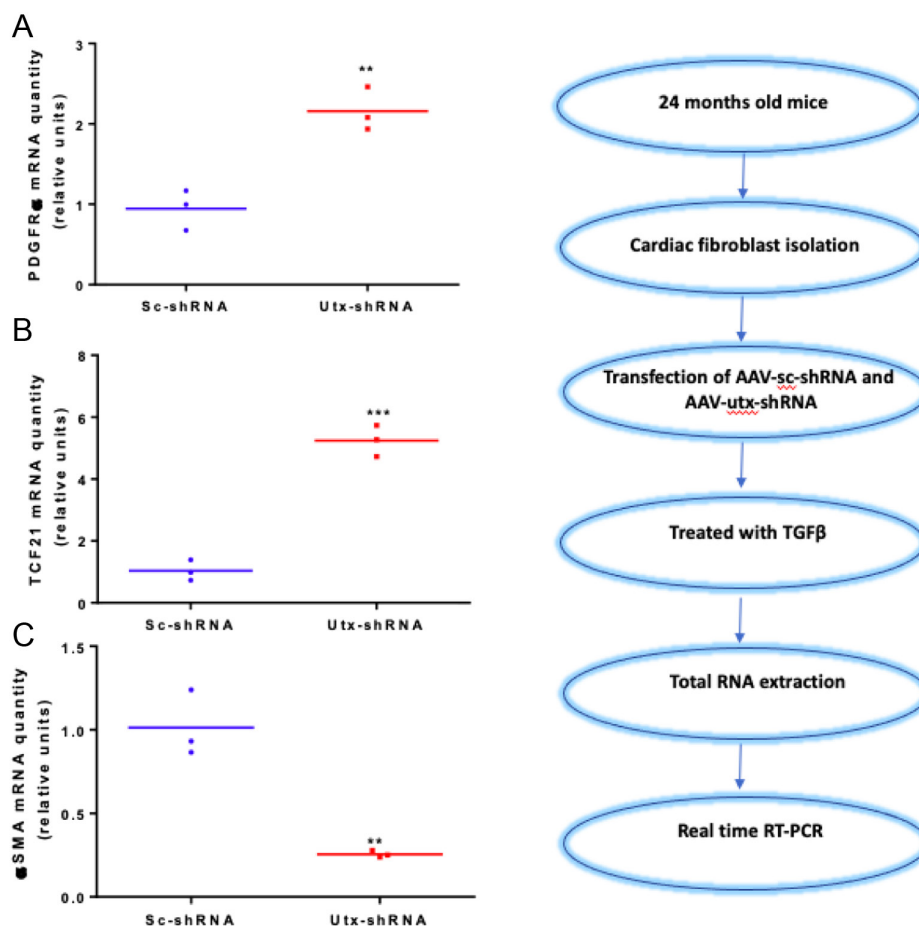

Figure 6. Ex vivo detection of PDGFRα, TCF21, and αSMA by real-time RT-PCR. (A): Relative PDGFRα mRNA level normalized by GAPDH. (B): Relative TCF21 mRNA level normalized by GAPDH. (C): Relative αSMA mRNA level normalized by GAPDH. Data are expressed as mean ± SEM. **$P < .01$, ***$P < .001$ vs. AAV-sc-shRNA-treated control mice, n = 3. AAV, adeno-associated virus; GAPDH, glyceraldehyde 3-phosphate dehydrogenase; PDGFRα, platelet-derived growth factor receptor alpha; RT-PCR, real-time polymerase chain reaction; αSMA, alpha smooth muscle actin; TCF21, transcription factor 21; shRNA, short hairpin RNA.

Li et al. Silencing of UTX and Cardiac Fibrosis

Anatol J Cardiol 2023; 27(7): 398-407

myofibroblasts contribute fibroblasts-to-myofibroblasts trans-differentiation. The main cellular effectors of fibrosis are the myofibroblasts.[31] Multiple factors are involved in the trans-differentiation of fibroblasts-to-myofibroblasts, including inflammation, chemokine, and cytokine secretion, consequently upregulating TGFβ secretion. Transforming growth factor beta upregulated and activated in fibrotic diseases and modulates fibroblast phenotype and function, inducing myofibroblast trans-differentiation.[32] The results from current study are consistent with these data, which aging-associated cardiac fibrosis caused collagen deposition, αSMA formation and TGFβ upregulation. Silencing of UTX abolished collagen deposition, αSMA formation, and TGFβ upregulation. Meanwhile, it upregulated expression of mature fibroblast marker TCF21 and PDGFRα. Mechanistically, ex vivo study confirmed that silencing of UTX in cellular level achieved a similar result (Figure 4E). These findings indicate that epigenetic regulation is involved in cardiac fibrosis. Silencing of UTX using AAV vector may serve as a target gene therapy for prevention of aging-associated cardiac fibrosis.

Adeno-associated virus vector is an FDA approved vector for clinical gene therapy. The excellent safety profiles, together with the high efficiency of transduction of a broad range of target tissues, have established AAV vector as the platform of choice for *in vivo* gene therapy.[33]

Adeno-associated viruses infect both dividing and nondividing cells and remain latent in the host cell DNA by integration into specific chromosomic loci (adeno-associated virus integration sites) unless a helper virus provides the functions for its replication.[34] The limitation of AAV vector is the insertion limitation of target gene. Short hairpin RNA sequence (20-24 bp) is an artificial RNA molecule with a tight hairpin turn that can be used to silence target gene expression via RNA interference (RNAi).[35,36] Thus, AAV is a suitable vector for shRNA gene delivery. This study may serve as a novel avenue for gene therapy in cardiac fibrosis.

CONCLUSIONS

Silencing of UTX by AAV-utx-shRNA attenuated aging-associated cardiac remodeling via blocking fibroblasts-to-myofibroblasts trans-differentiation. Interventional control of cardiac fibrosis may be a new preventive and therapeutic strategy for cardiac dysfunction. AAV-utx-shRNA provides an effective therapeutic approach for the treatment of aging-associated cardiac fibrosis and dysfunction. The detailed mechanism of UTX in communications with cardiac fibroblasts in cardiac hypertrophy, fibrosis, and cardiac dysfunction will be explored.

Author Contributions: C.L. – Conceptualization, Writing – Original Draft, Formal analysis; T.L., D.L., D.S., H.S. – Resources, Investigation; S.Y., Z.Z., Z.Q. – Validation; K.S. – Methodology, Writing – Review & Editing, Funding acquisition, Project administration.

REFERENCES

1. Roadmap Epigenomics Consortium, Kundaje A, Meuleman W, et al. Integrative analysis of 111 reference human epigenomes. *Nature*. 2015/02/20;518(7539):317-330. [CrossRef]
2. Bauer AJ, Martin KA. Coordinating regulation of gene expression in cardiovascular disease: interactions between chromatin modifiers and transcription factors. *Front Cardiovasc Med*. 2017/04/22;4:19. [CrossRef]
3. Jin C, Li J, Green CD, et al. Histone demethylase UTX-1 regulates *C. elegans* life span by targeting the insulin/IGF-1 signaling pathway. *Cell Metab*. 2011/08/02;14(2):161-172. [CrossRef]
4. Lan F, Bayliss PE, Rinn JL, et al. A histone H3 lysine 27 demethylase regulates animal posterior development. *Nature*. 2007/09/14;449(7163):689-694. [CrossRef]
5. Agger K, Cloos PA, Christensen J, et al. UTX and JMJD3 are histone H3K27 demethylases involved in HOX gene regulation and development. *Nature*. 2007/08/24;449(7163):731-734. [CrossRef]
6. Maures TJ, Greer EL, Hauswirth AG, Brunet A. The H3K27 demethylase UTX-1 regulates C. elegans lifespan in a germline-independent, insulin-dependent manner. *Aging Cell*. 2011/08/13; 10(6):980-990. [CrossRef]
7. Scaffidi P, Misteli T. Reversal of the cellular phenotype in the premature aging disease Hutchinson-Gilford progeria syndrome. *Nat Med*. 2005/03/08;11(4):440-445. [CrossRef]
8. McCord RP, Nazario-Toole A, Zhang H, et al. Correlated alterations in genome organization, histone methylation, and DNA-lamin A/C interactions in Hutchinson-Gilford progeria syndrome. *Genome Res*. 2013;23(2):260-269. [CrossRef]
9. Trial J, Heredia CP, Taffet GE, Entman ML, Cieslik KA. Dissecting the role of myeloid and mesenchymal fibroblasts in age-dependent cardiac fibrosis. *Basic Res Cardiol*. 2017;112(4):34. [CrossRef]
10. MacKenna D, Summerour SR, Villarreal FJ. Role of mechanical factors in modulating cardiac fibroblast function and extracellular matrix synthesis. *Cardiovasc Res*. 2000/04/25;46(2):257-263. [CrossRef]
11. Sun Y, Kiani MF, Postlethwaite AE, Weber KT. Infarct scar as living tissue. *Basic Res Cardiol*. 2002/08/30;97(5):343-347. [CrossRef]
12. Anversa P, Hiler B, Ricci R, Guideri G, Olivetti G. Myocyte cell loss and myocyte hypertrophy in the aging rat heart. *J Am Coll Cardiol*. 1986/12/01;8(6):1441-1448. [CrossRef]
13. Anversa P, Palackal T, Sonnenblick EH, Olivetti G, Meggs LG, Capasso JM. Myocyte cell loss and myocyte cellular hyperplasia in the hypertrophied aging rat heart. *Circ Res*. 1990/10/01;67(4): 871-885. [CrossRef]
14. Tallquist MD, Molkentin JD. Redefining the identity of cardiac fibroblasts. *Nat Rev Cardiol*. 2017/04/25;14(8):484-491. [CrossRef]
15. Acharya A, Baek ST, Huang G, et al. The bHLH transcription factor Tcf21 is required for lineage-specific EMT of cardiac fibroblast progenitors. *Development*. 2012/05/11;139(12):2139-2149. [CrossRef]

16. Rinn JL, Chang HY. Genome regulation by long noncoding RNAs. *Annu Rev Biochem*. 2012/06/06;81:145-166. [CrossRef]

17. Olson LE, Soriano P. Increased PDGFRalpha activation disrupts connective tissue development and drives systemic fibrosis. *Dev Cell*. 2009/02/17;16(2):303-313. [CrossRef]

18. Hermens WT, ter Brake O, Dijkhuizen PA, et al. Purification of recombinant adeno-associated virus by iodixanol gradient ultracentrifugation allows rapid and reproducible preparation of vector stocks for gene transfer in the nervous system. *Hum Gene Ther*. 1999/08/14;10(11):1885-1891. [CrossRef]

19. Rohr UP, Wulf MA, Stahn S, Steidl U, Haas R, Kronenwett R. Fast and reliable titration of recombinant adeno-associated virus type-2 using quantitative real-time PCR. *J Virol Methods*. 2002/10/09;106(1):81-88. [CrossRef]

20. Feng M, Whitesall S, Zhang Y, Beibel M, D'Alecy L, DiPetrillo K. Validation of volume-pressure recording tail-cuff blood pressure measurements. *Am J Hypertens*. 2008/10/11;21(12): 1288-1291. [CrossRef]

21. Rohrer DK, Hartong R, Dillmann WH. Influence of thyroid hormone and retinoic acid on slow sarcoplasmic reticulum Ca2+ ATPase and myosin heavy chain alpha gene expression in cardiac myocytes. Delineation of cis-active DNA elements that confer responsiveness to thyroid hormone but not to retinoic acid. *J Biol Chem*. 1991;266(13):8638-8646.

22. Yu B, Yu M, Zhang H, Xie D, Nie W, Shi K. Suppression of miR-143-3p contributes to the anti-fibrosis effect of atorvastatin on myocardial tissues via the modulation of Smad2 activity. *Exp Mol Pathol*. 2020;112:104346. [CrossRef]

23. Barsha G, Denton KM, Mirabito Colafella KM. Sex- and age-related differences in arterial pressure and albuminuria in mice. *Biol Sex Differ*. 2016/11/30;7:57. [CrossRef]

24. Boyle AJ, Shih H, Hwang J, et al. Cardiomyopathy of aging in the mammalian heart is characterized by myocardial hypertrophy, fibrosis and a predisposition towards cardiomyocyte apoptosis and autophagy. *Exp Gerontol*. 2011/03/08;46(7):549-559. [CrossRef]

25. Olivetti G, Melissari M, Capasso JM, Anversa P. Cardiomyopathy of the aging human heart. Myocyte loss and reactive cellular hypertrophy. *Circ Res*. 1991;68(6):1560-1568. [CrossRef]

26. Biernacka A, Frangogiannis NG. Aging and cardiac fibrosis. *Aging Dis*. 2011/08/13;2(2):158-173.

27. Pieraggi MT, Bouissou H, Angelier C, Uhart D, Magnol JP, Kokolo J. [The fibroblast]. *Ann Pathol*. 1985/01/01;5(2):65-76.

28. Willems IE, Havenith MG, De Mey JG, Daemen MJ. The alpha-smooth muscle actin-positive cells in healing human myocardial scars. *Am J Pathol*. 1994/10/01;145(4):868-875.

29. Kong P, Christia P, Frangogiannis NG. The pathogenesis of cardiac fibrosis. *Cell Mol Life Sci*. 2014;71(4):549-574. [CrossRef]

30. Rog-Zielinska EA, Norris RA, Kohl P, Markwald R. The living scar--cardiac fibroblasts and the injured heart. *Trends Mol Med*. 2016/01/19;22(2):99-114. [CrossRef]

31. Wipff PJ, Rifkin DB, Meister JJ, Hinz B. Myofibroblast contraction activates latent TGF-beta1 from the extracellular matrix. *J Cell Biol*. 2007;179(6):1311-1323. [CrossRef]

32. Biernacka A, Dobaczewski M, Frangogiannis NG. TGF-beta signaling in fibrosis. *Growth Factors*. 2011/07/12;29(5):196-202. [CrossRef]

33. Colella P, Ronzitti G, Mingozzi F. Emerging issues in AAV-mediated in vivo gene therapy. *Mol Ther Methods Clin Dev*. 2018/01/13;8:87-104. [CrossRef]

34. Balakrishnan B, Jayandharan GR. Basic biology of adeno-associated virus (AAV) vectors used in gene therapy. *Curr Gene Ther*. 2014/03/05;14(2):86-100. [CrossRef]

35. Paddison PJ, Caudy AA, Bernstein E, Hannon GJ, Conklin DS. Short hairpin RNAs (shRNAs) induce sequence-specific silencing in mammalian cells. *Genes Dev*. 2002/04/18;16(8):948-958. [CrossRef]

36. Brummelkamp TR, Bernards R, Agami R. A system for stable expression of short interfering RNAs in mammalian cells. *Science*. 2002/03/23;296(5567):550-553. [CrossRef]
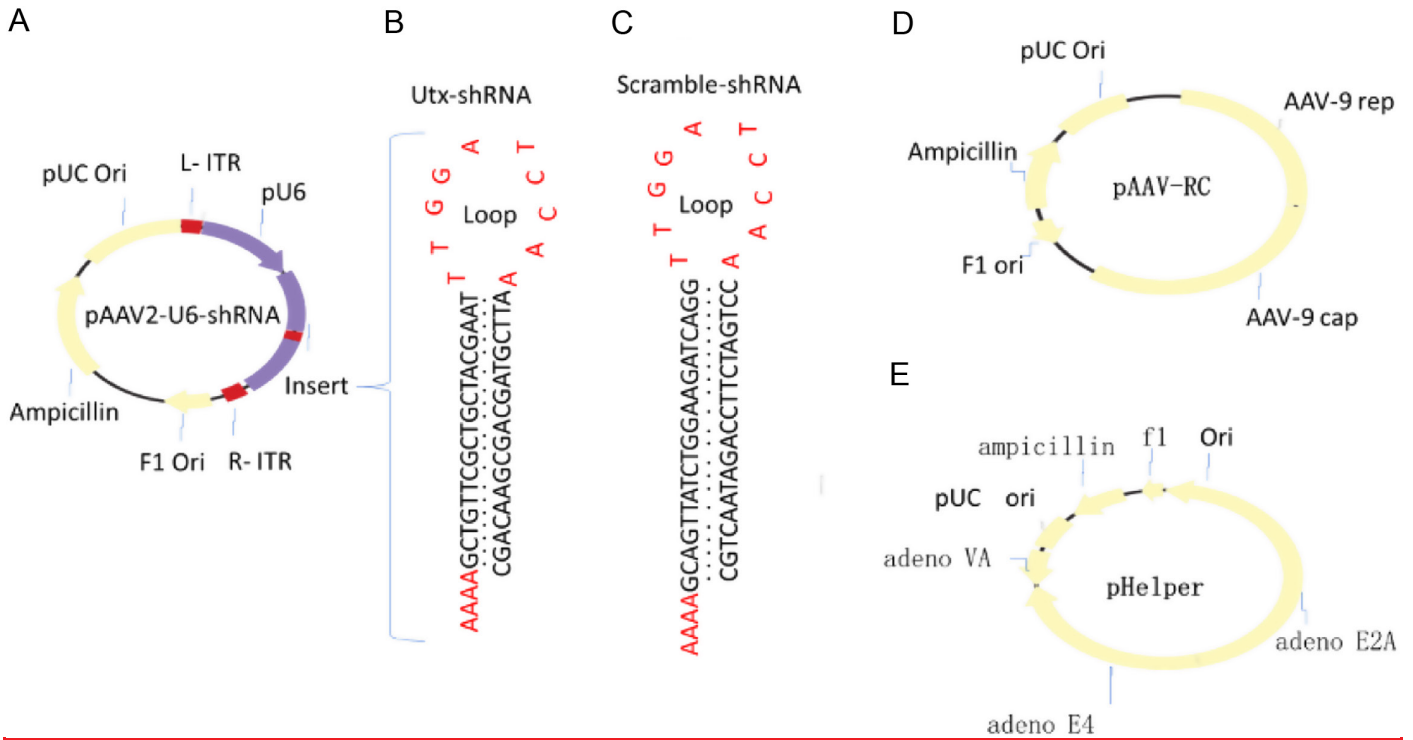
Supplementary Figure 1. Construction of recombinant AAV2/9 vector. A: AAV-2 backbone vector. B: Structure of utx-shRNA-2. C: Structure of sc-shRNA (control). D: AAV-9 vector for packaging AAV2/9. E: Helper vector for packaging AAV2/9.
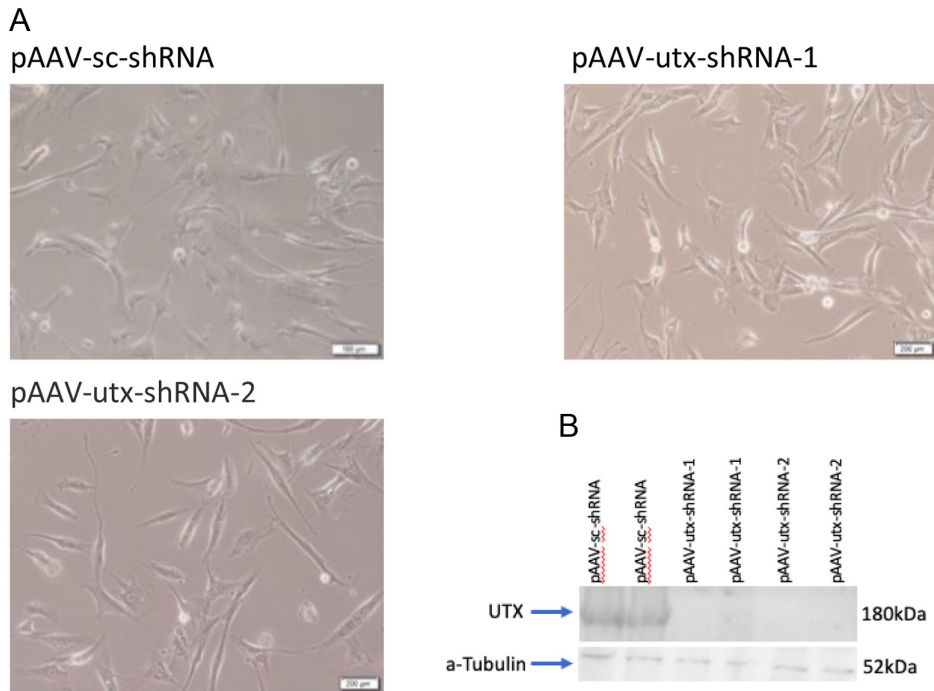
Supplementary Figure 2. Inhibition efficiency of pAAV-utx-shRNAs in isolated cardiac fibroblasts. A: Representative images of isolated cardiac fibroblasts transfected with pAAV-sc-shRNA and pAAV-utx-shRNAs. B: Western blot analysis of UTX expression in isolated cardiac fibroblasts.